DEVELOPMENT OF INPUT POWER COUPLER FOR ERL MAIN LINAC IN JAPAN

Hiroshi Sakai#, Takaaki Furuya, Shogo Sakanaka, Takeshi Takahashi, Kensei Umemori,
KEK, Tsukuba, Ibaraki, 305-0801, Japan,
Atsushi Ishii, Norio Nakamura, Kenji Shinoe, ISSP, Univ. of Tokyo, Kashiwa, Chiba, 277-8581, Japan,
Masaru Sawamura, JAEA-ERL, Tokai, Naka, Ibaraki, 319-1195, Japan

Abstract

We started to develop an input coupler for a 1.3GHz ERL superconducting cavity for ERL main linac[1,2]. Required input power is about 20kW for the cavity acceleration field of 20MV/m and the beam current of 100mA in energy recovery operation. The input coupler is designed based on the STF-BL input coupler [3] and some modifications are applied for the CW 20kW power operation. We fabricated input coupler components such as ceramic windows and bellows and carried out the high-power test of the components by using a 30kW IOT power source and a test stand constructed.

INTRODUCTION

An input coupler is one of the important items of the superconducting cavity for ERL operation [1,2]. Then, we now design the input power coupler for the main linac. Thanks to the mechanism of energy recovery, we can reduce the input power of the main linac. However, the minimum input power will be restricted by the cavity detuning due to the microphonics from the cryomodule.

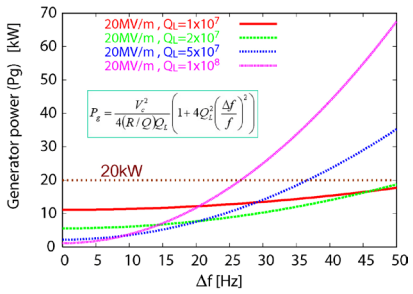

Figure.1: Δf vs input power on several Q_L's.

Fig.1 shows the relation between the cavity detuning (Δf) and the input power corresponding to the several loaded Q-values (Q_L) of accelerating field of 20 MV/m. In our main linacs, the maximum input power of 20 kW for the large cavity detuning of Δf=50Hz is required under Q_L=2x10^7.

Frequency	1.3GHz
Accelerating voltage	15~20MV/m
Input power	Max 20kW
Loaded Q (Q_L)	5x10^6 ~ 2x10^7(variable)

Table 1: Parameters of input coupler for main linac.

Fig.2 shows the design of the input power coupler for our main linac. Our input power coupler is based on the coaxial antenna type couplers for a prototype of STF-BL coupler [3]. This prototype coupler used the two choke-mode ceramic windows and was already powered in a test bench. It successfully passed through 1MW pulsed peak power on a test bench. This is one of the reasons why we select this type of coupler. The following major modifications were made to meet our requirements.

- Change the impedance from 50Ω to 60Ω to reduce the heat load of inner conductor. Furthermore forced air cooling was applied to inner conductor.
- Purity of ceramic material was changed from 95% to 99.7% to reduce the heat load of ceramic.
- Cold ceramic size is same as warm one.
- Variable coupling was applied from Q_L = 5x10^6 to 2x10^7 for the short pulse conditioning of input power coupler in commissioning.
- In order to absorb the heat load of inner conductor, 80K thermal anchor is applied on cold window and 5K thermal anchor is also equipped for the reduction of the static loss to 2K.

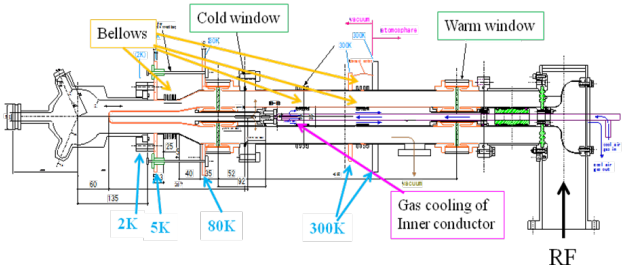

Figure 2: Schematic design of input coupler for main linac

Heat load per cavity	2K	5K	80K
Dynamic loss (20kW SW)	-	3.3W	31.9W
Static loss	0.3W	1W	15.5W
Total	0.3W	4.25W	47.4W

Table 2: Estimated heat load of input coupler

Table 2 shows the estimated heat load of input coupler by applying the 20kW CW input power with standing wave. Dynamic load is high comparing to the static loss at 5K and 80K thermal anchor. In our case, static loss of 80K is also not small because the length between the air floe region of inner conductor and 80K thermal anchor is short. Thanks to the two type of thermal anchor, heat leak to 2K is reduced down to 0.3W.

It is important for an input coupler to check the heat load and temperature rise. Especially to test the key components of the input power coupler such as ceramic

sakai.hiroshi@kek.jp

windows and bellows, we made a test stand as shown in Fig.3. In detail, we explain next section.

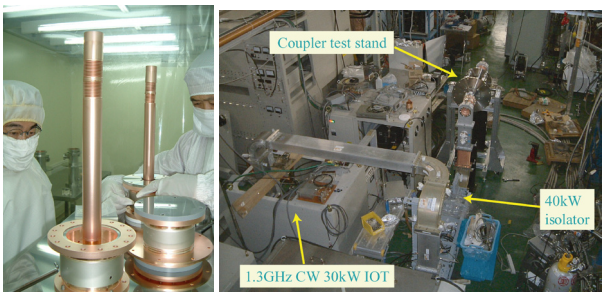

Figure 3: (Left) Pictures of cold and warm windows. (Right) Setup of test stand.

HIGH POWER TEST IN ATMOSPHERIC CONDITION

Fig.4 shows schematic diagram of the high power test stand. We fabricated two warm windows with bellows and two cold windows as shown in Fig.3. In test stand, warm windows with bellows sandwiched one cold window. Three windows were assembled in the class 10 clean room after rinsed by ultra-pure water. The RF power went through these three windows from 30kW IOT via doorknob exchangers and finally dumped at the dummy load. Temperatures of bellows and three windows were monitored. Especially, in order to monitor the temperature rise of bellows of inner conductor precisely, we set the thermo coupler at three different positions; one is set at the front of bellows, another is the middle of bellows and the other is the end of bellows as shown in Fig.5. These thermo couplers were connected with Au brazing to obtain the tight connection. Transmitted and reflected RF power are also measured before and after the three windows and after the IOT. The inner conductor and bellows were cooled via rod by air compressor and the amount of air flow was monitored.

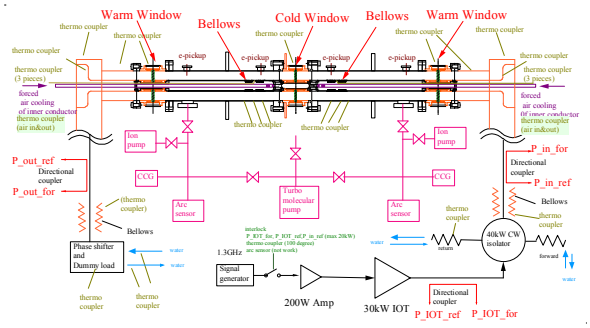

Figure.4: schematic diagram of test stand

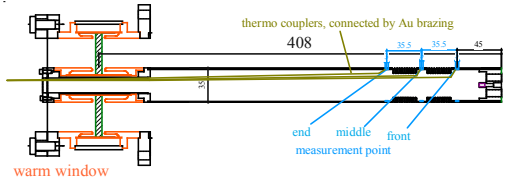

Figure.5: Details of warm window. Three thermo couplers are set inside the inner conductor near bellows

First we measured the temperature rise with and without forced air cooling during 1kW power with travelling wave. We wanted to check the heat loads of the bellows and ceramic window. Therefore, we did not pump the vacuum between windows on this test stand. Each temperature rise is 16K and 4K without and with cooling as shown in the left figure of Fig.6, respectively. We note that the temperature rise of bellows of inner conductor was measured and suppressed by forced air cooling by a factor of four at this high power test stand by applying 64l/min air flow. This result almost agrees well with the calculation as shown in the right figure of Fig.6. Then the forced air cooling works well to the bellows.

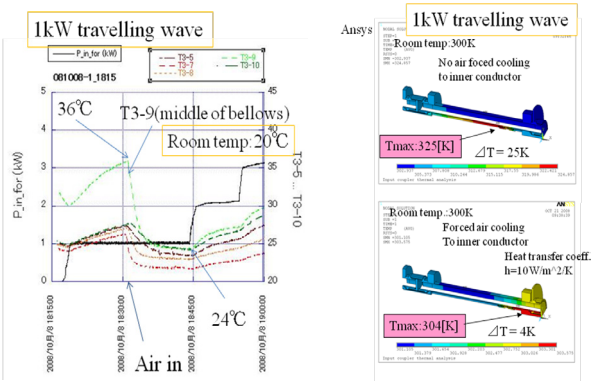

Figure 6: (Left) 1kW power test. Green line shows the temperature rise of middle of bellows. (Right) Simulation of temperature rise w/wo air flow of inner conductor

After that, we fed the RF power up to 20kW under the atmospheric condition with the 64l/min air cooling. Fig.7 shows the results of the high power test. When the power increases above 8kW, the sudden temperature rise was observed at cold windows as shown in the left figure of Fig.7. Especially, sudden temperature rise was correlated with power loss through the three ceramic windows.

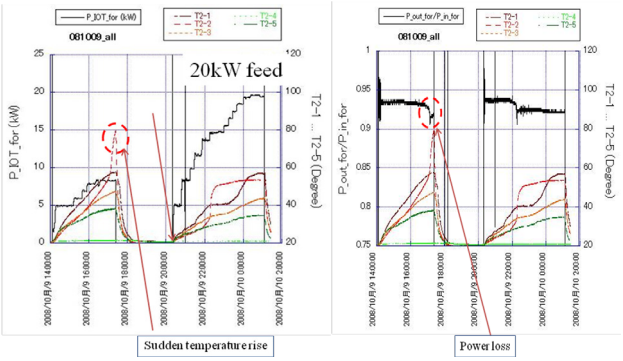

Figure 7: Results of 20kW power test (Left) Red, brown and orange lines show the temperature of cold, warm (upper) and (down) ceramic windows, respectively. Black line shows the power of IOT. (Right) Red, brown and orange is same as left figure, black one is power ratio after and before the windows.

In order to investigate the sudden temperature rise in detail, we measured the S-parameters while changing the temperature by adding heat load through the heater to cold window. By measuring the S_{21}, we found the peak at 1.305GHz. And we found the peak shifted to 1.3GHz when temperature increased as shown in Fig.8. From these results, this unexpected peak might induce the power loss and result in the sudden temperature rise of cold ceramic windows. After the high power test, we open the test stand. We found that cold ceramic window was broken. Fig.9 shows the broken profile of cold window. We suspected that big temperature rise was occurred in cold windows. We note that warm windows were not broken and bellows has no change and damage after high power test feeding 20kW CW travelling wave

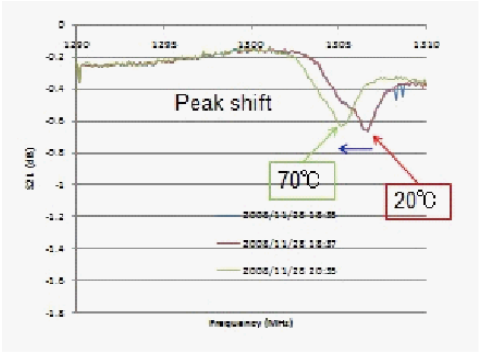

Figure 8: Results of S_{21} of low level measurement through 3 ceramic windows when the temperature was increased. Red and green lines show the S_{21} at 20C° and 70C° at outside of the cold window, respectively.

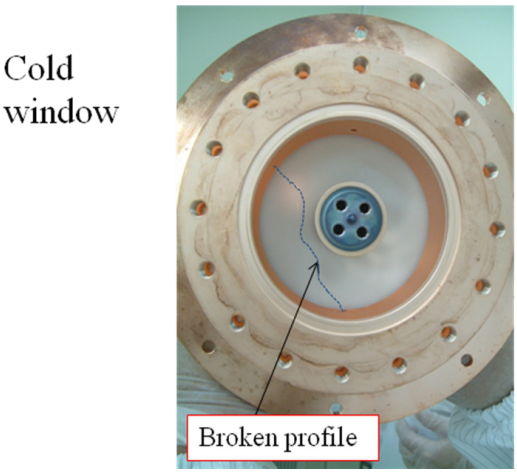

Figure 9: Picture of cold window with broken profile.

Why did cold ceramic window break? To check what produces the unexpected peak near 1.3GHz, we apply the low level measurement of cold ceramic window only after cold window was broken. We found the sharp peak on 1.305GHz as shown in Fig.10. This peak was also found on another cold window of same size. We found that this unexpected peak was intrinsic of cold/warm ceramic window. To survey the detail of property of this unexpected peak, we calculate the eigenmode of cold/warm ceramic window by using HFSS and MW-stdio simulation code. And we also found that the resonance peak near 1.3GHz, which represents the TE dipole mode as shown in Fig.11. We suspect that this dipole mode might be measured unexpected peak. Fortunately, the frequency of this dipole mode depends on the thickness of ceramic window as shown in Fig.11. To escape this dipole mode, we plan to modify the ceramic window by changing the thickness of ceramic down to 5.4mm, which is thinner than present thickness of 6.2mm.

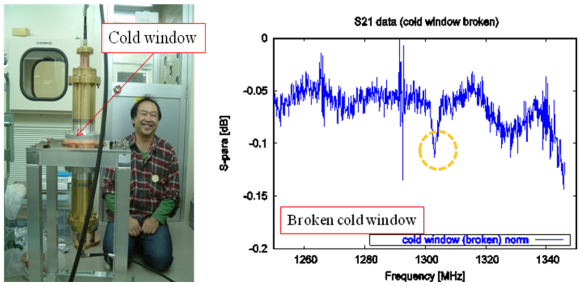

Figure 10: (Left) Setup of low level measurement of the cold window. (Right) Result of measurement.

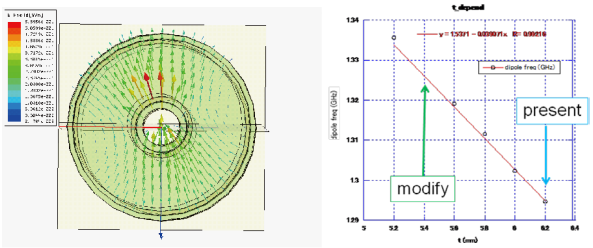

Figure 11: (Left) Calculated dipole mode standing on the ceramic window near 1.3GHz by HFSS. (Right) frequency dependence of dipole mode corresponding to the thickness of ceramic by HFSS.

HIGH POWER TEST UNDER VACUUM CONDITION WITH STANDING WAVE

Only warm windows with bellows were survived for previous three-ceramic window high power test. Next we tried to test the high power test in vacuum condition by using warm window only. Fig.12 shows the setup of high power test of warm window with standing wave. Each inner side of warm window with bellows, end plate and outer conductor was rinsed by ultra-pure water. After drying these components, we assembled at class 10 clean room. The volume between warm window and end plate were pumped by an ion pump and the vacuum pressure was measured by CCG. After baking at 150 C° for 24 hours, the vacuum pressure of $6x10^{-7}$ Pa was achieved before high power test. RF power was fed into warm windows from 30kW IOT via doorknob exchangers and reflected by end plate. Therefore standing wave was

excited at warm window and bellows. Calculated magnetic field was shown in Fig.13 on this setup. The peak of magnetic field of standing wave will be set on the middle of bellows and warm ceramic window in this setup. Temperatures of bellows at the same three positions of Fig.5 and warm window were monitored. Transmitted RF power (Pin_for) and reflected RF power (Pin_ref) are also measured before the warm windows and after the IOT. The inner conductor and bellows were cooled via rod by air compressor and the amount of air flow was monitored. Arc sensor was set on the end plate. Two pick-up probes were set to see the electrons in vacuum; one was set near the warm window and another near the end plate.

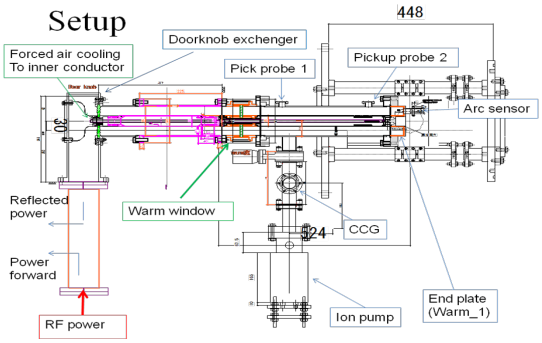

Figure.12: Setup of warm window high power test with standing wave.

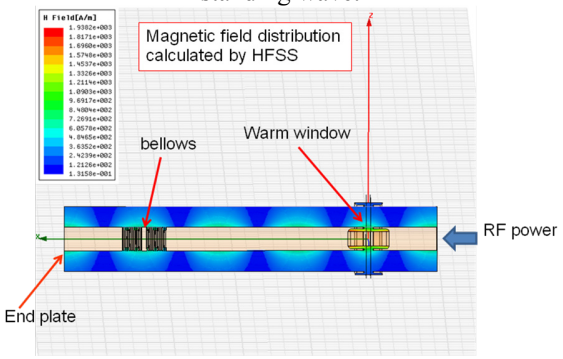

Figure.13: calculated magnetic field distribution of this setup by HFSS.

We apply the RF power to warm window. We smoothly increased the RF power until 14.5kW. We measure the temperature rise by changing the amount of air flow ratio of inner conductor. Fig. 14 shows the typical temperature rise of bellows parts on different air flow conditions. First we took the data of 5kW and 10kW standing wave by inserting the 64l/min air flow to inner conductor. Temperature rise of the middle point of bellows became 96K. at 10kW. Next we increased the air flow up to 92l/min. The temperature rise was decreased to 62K as shown in the left figure of Fig.14. After that we also measured the temperature rise without air cooling with 1kW standing wave condition as shown in the right figure of Fig.14. Temperature rise was 116K at the middle of bellows. Fig.15 shows the results of the temperature rise vs power flow at different air flows. Temperature rise is almost linear to the input power. In all cases, the temperature rise of middle point is larger than the end of bellows. This means that, in standing wave, magnetic current at the middle of bellows produces much heat load. Especially, if we did not apply air cooling, this difference between the middle and end of bellows much increased because of the small thermal conductivity of bellows. We observed few difference between the air temperature after passing through inner conductor and the end of bellows.

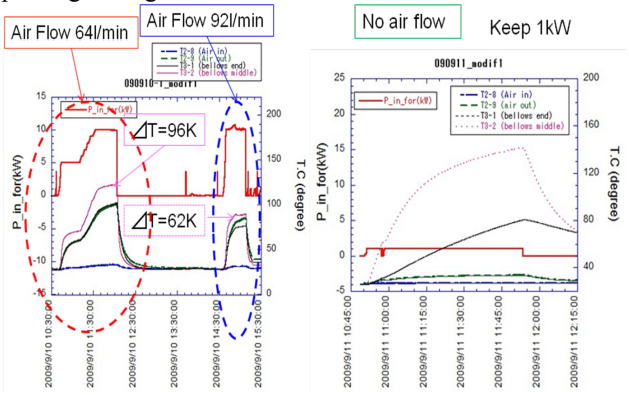

Figure.14: Typical temperature rise of bellows parts on different air flow conditions. (Left) Keep 5kW and 10kW by applying the 64l/min air flow and keep 10kW the 92l/min air flow. Red line shows the input power. Pink, black lines show the temperature of bellows middle and end points, respectively. Blue and black lines show the temperatures of air before and after going through the inner conductor. (Right) No air flow to the inner conductor. The definitions of lines are same as left figure.

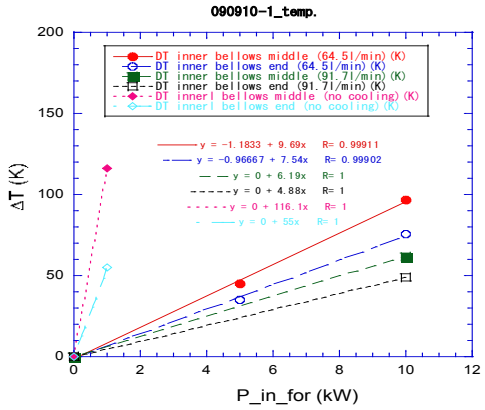

Figure.15: Input power (Pin_for) vs temperature rise on different air flow conditions. Measured point is the middle and end point of bellows.

Air flow (l/min)	ΔT/ΔP Bellows middle (K/kW)	ΔT/ΔP Bellows end (K/kW)
0	116.1	55
64.5	9.7	7.5
91.7	6.2	4.9

Table 3: Summary of the ratio of temperature rise (ΔT) to transmitted RF power to warm window (ΔP) of two bellows points at different air flows.

To see the effect of air flow, we summarized the rate of temperature rise (ΔT) to transmitted RF power to warm window (ΔP), which is the slope of Fig.15, of two bellows points at different air flows in Table.3. These values are twice larger than the previous three ceramic high power test because of the difference of the case of travelling wave and standing wave. RF Power travelled on the coupler test stand twice at standing wave. ΔT/ΔP is in inverse proportion to the amount of air flow. The forced air cooling works well to reduce the heat load. We compared CW high power test of TTF-III coupler test, which were tested on HoBiCaT and tested forced air cooling to inner conductor [4]. Our result is about 2-3 times larger than CW test of TTF-III coupler. One of the reason is the length of our inner conductor is larger than TTF-III coupler. In our case, we add the extension of inner conductor. We will modify to reduce the inner conductor to reduce the heat load and compare these results.

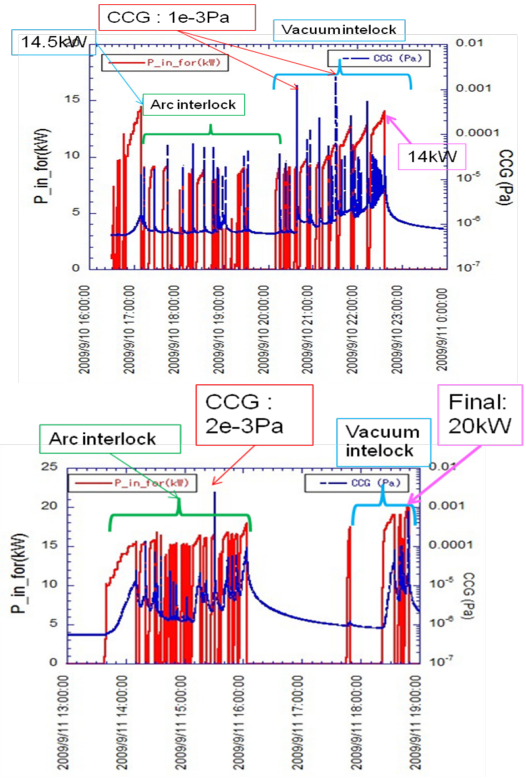

Figure.16: History of the power processing up to 20kW. (up) 10-15kW. (down) 15-20kW. Red lines show input power and blue lines show the vacuum pressure.

We continued to feed into power to test stand. At 14.5kW, suddenly arc and vacuum interlock works. Fig.16 shows the processing history up to 20kW. After that many arc and vacuum interlocks worked at 9kW level. We met the several vacuum interlock to 15kW. Many arc and vacuum interlocks also worked at 15-16kW level. And finally we reach the 20kW. When the arc interlock works, we found the electron signal as shown in Fig.17. Signal of probe near warm ceramic is much higher than probe near end plate. This shows that processing of the ceramic window is done. Power loss was not observed compared to the previous three ceramic window high power test. No leak and damage of ceramic windows and bellows were observed at this high power test.

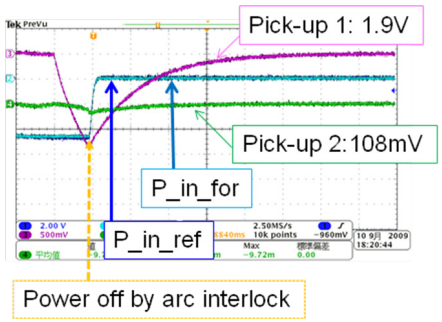

Figure.17: Signals come from two pick-up probes.

SUMMARY

We designed the 20kW input power coupler for ERL main linac. We made the high power test stand and did the component tests such as ceramic windows and bellows in atmospheric condition. Measurement results of temperature rise of bellows almost agree well with the calculation. We found the sudden temperature rise was appeared on cold ceramic windows, which results in the break of the cold window. After the low level measurement, we found the peak at 1.305GHz, which is same as the simulation of the unexpected dipole mode. From these results, sudden temperature rise might be affected by this unexpected mode. We note that bellows and warm windows works well under vacuum condition at high power test up to 20kW with standing wave. The temperature rise is slightly larger at middle of bellows. But forced air cooling works well up to 20kW standing wave. We also plan to modify the ceramic window by changing the thickness of ceramic and finally will make the first input coupler for main linac in this year.

ACKNOLEDGEMENT

We thank S.Noguchi, E.Kako from KEK, and S.Belmestnykh from Cornell Univ. for the help of designing of input coupler and test stand. We also thank N.Ohuchi from JAEA for assembling the test stand.

REFERENCE

[1] S.Sakanaka, et.,al, “Status of the energy recovery linac project in Japan”, PAC’09, Vancouver, May (2009).

[2] K.Umemori et al., “Status of 9-cell superconducting cavity development for ERL project in Japan”, in these proceedings, TUPPO055.

[3] E.Kako et al, “Advances and performance of input coupler at KEK” in these proceedings, THOBAU02.

[4] W.Anders et al., “CW operation of superconducting TESLA cavities”, Proceedings of 13-th SRF Workshop, Beijing, (2007)